Electronic Supplementary Material (ESI) for Green Chemistry.

Supporting Information

Bimetallic Single Atom Promoted α-MnO_2 for Enhanced Catalytic Oxidation of 5-Hydroxymethylfurfural

*Xuemei Liao [a], Mengdie Guo [a], Wei Tang [a], Changwen Liu [a], Wei Luo [b], Lei Tan [b], Tomohiro Noguchi [c], Miho Yamauchi [c, d, e], Yonghui Zhao [f], Xiaopeng Li [b,] **

[a] College of Food and Biological Engineering, Xihua University, Chengdu 610039, Sichuan, China

[b] State Key Laboratory for Modification of Chemical Fibers and Polymer Materials & College of Materials Science and Engineering, Donghua University, No. 2999 North Renmin Road, Songjiang District, Shanghai 201620, China

[c] Institute for Materials Chemistry and Engineering, Motooka 744, Nishi-ku, Fukuoka 819-0395, Japan (IMCE), Kyushu University, Motooka 744, Nishi-ku, Fukuoka 819-0395, Japan

[d] Advanced Institute for Materials Research (AIMR), Tohoku University, 2-1-1 Katahira, Aoba-ku, Sendai, 980-8577, Japan

[e] Research Center for Negative Emissions Technologies (K-Nets), Kyushu University, Motooka 744, Nishi-ku, Fukuoka 819-0395, Japan

[f] CAS Key Laboratory of Low-Carbon Conversion Science and Engineering, Shanghai Advanced Research Institute (SARI), Chinese Academy of Sciences (CAS), No. 100, Haike Road, Pudong New District, Shanghai 201210, China

*Corresponding Author E-mail: xiaopeng.li@dhu.edu.cn

Experimental details:

Preparation of Ni_H/MnO_2:

Ni_H/MnO_2 catalyst was prepared by the impregnation method. The un-doped α-MnO_2 powder prepared by the hydrothermal method as described in the experimental part was added into the aqueous $Ni(NO_3)_2$ solution (30 mL of ultrapure water, 0.104g $Ni(NO_3)_2 \cdot 6H_2O$) under stirring for 1.5 h. Then the above suspension was evaporated in a water bath at 80 ^oC. The obtained brown-dark solid was dried in the oven overnight and finally calcined in a muffle furnace at 300 ^oC for 3 h.

Preparation of Pd_H/MnO_2 and $PdNi_H/MnO_2$

Pd_H/MnO_2 and $PdNi_H/MnO_2$ catalysts were synthesized by a one-step hydrothermal method. The procedures were the same as that of $PdNi/MnO_2$ sample. The addition amount of $Pd(NO_3)_2$ was 0.021g for Pd_H/MnO_2. For $PdNi_H/MnO_2$, The addition amounts of $Pd(NO_3)_2$ and $Ni(NO_3)_2$ were 0.007g and 0.104 g, respectively.

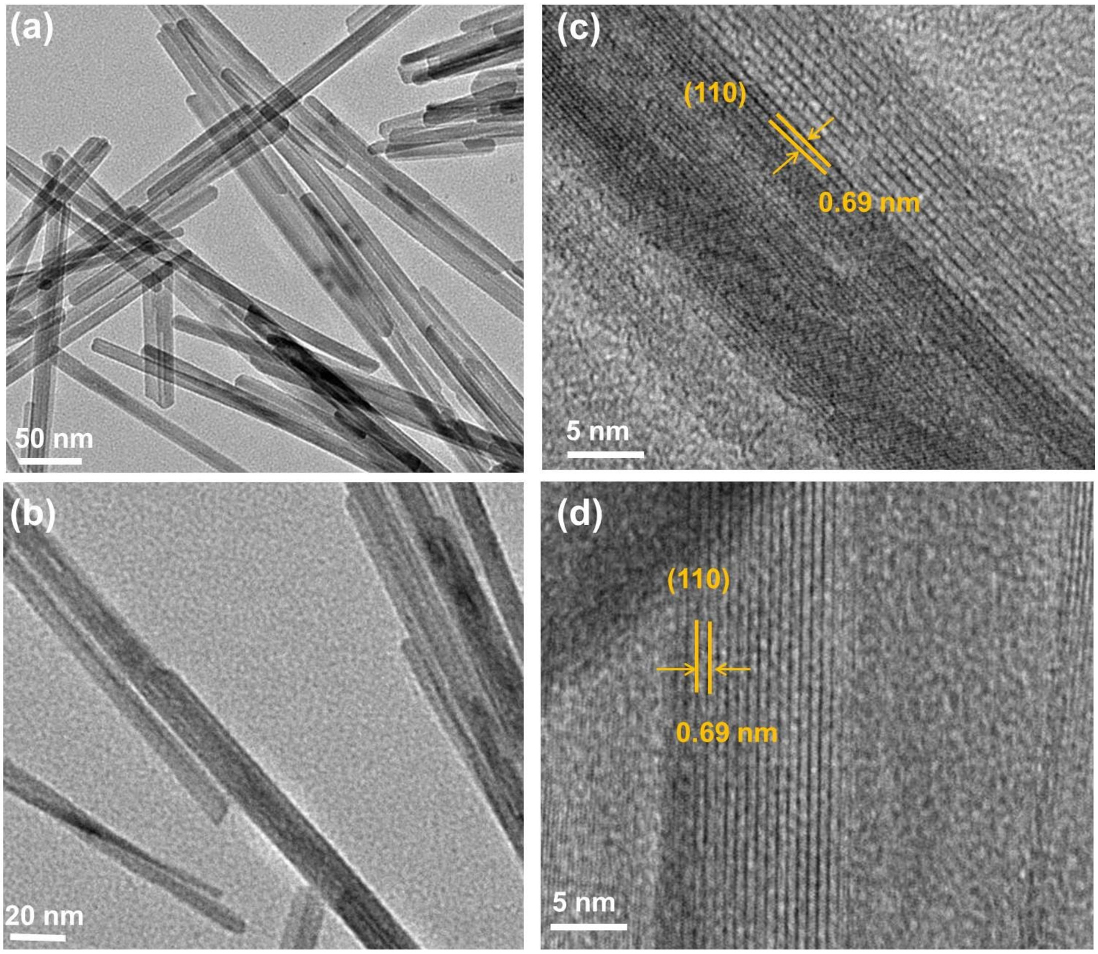

Figure S1. (a and b) TEM and (c and d) HRTEM images of non-doped MnO_2.

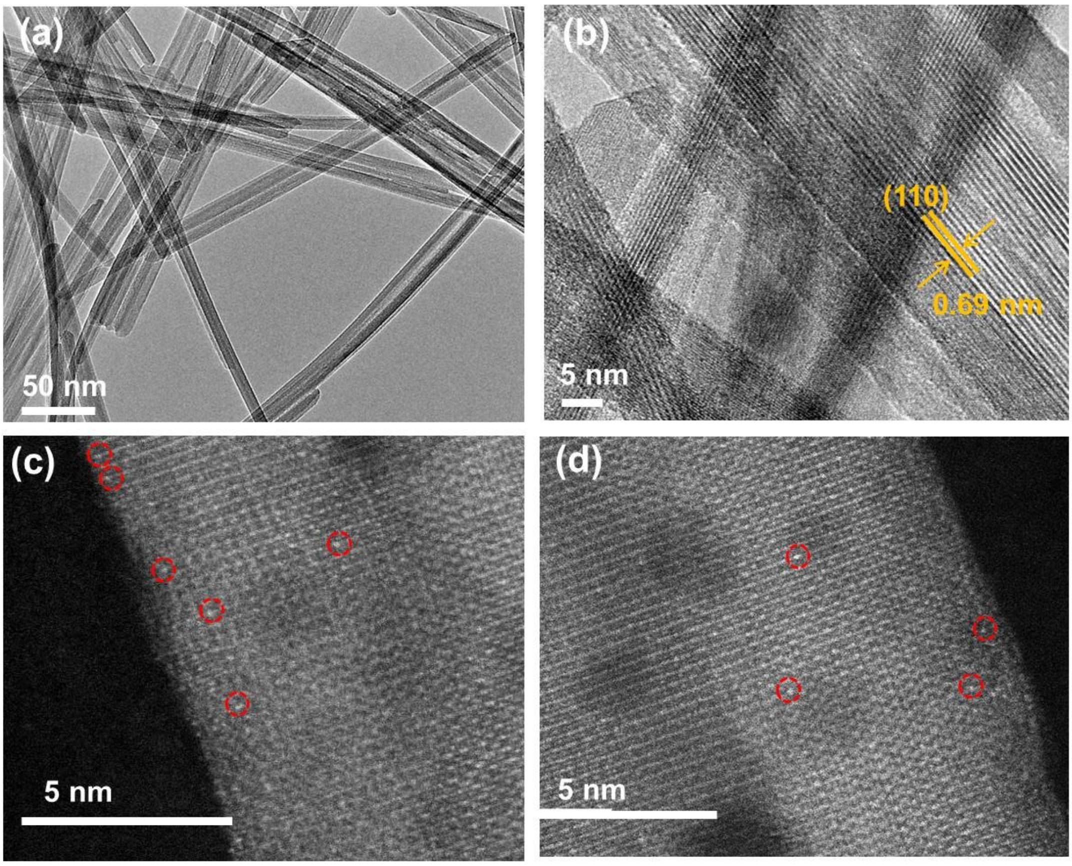

Figure S2. (a) TEM, (b) HRTEM, and (c-d) Sub-Ångström-resolution HAADF-STEM images of Pd/MnO_2. Red dotted circle highlights the presence of single Pd atom.

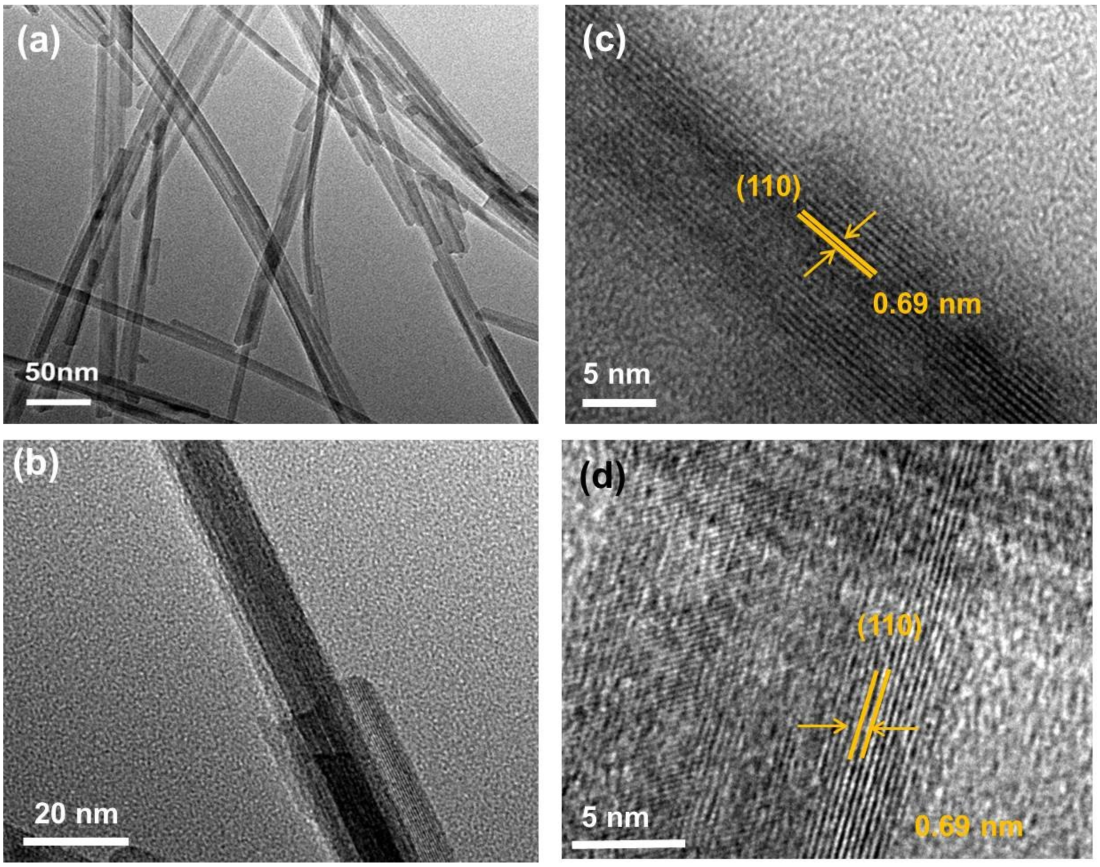

Figure S3. (a and b) TEM and (c and d) HRTEM images of Ni/MnO_2.

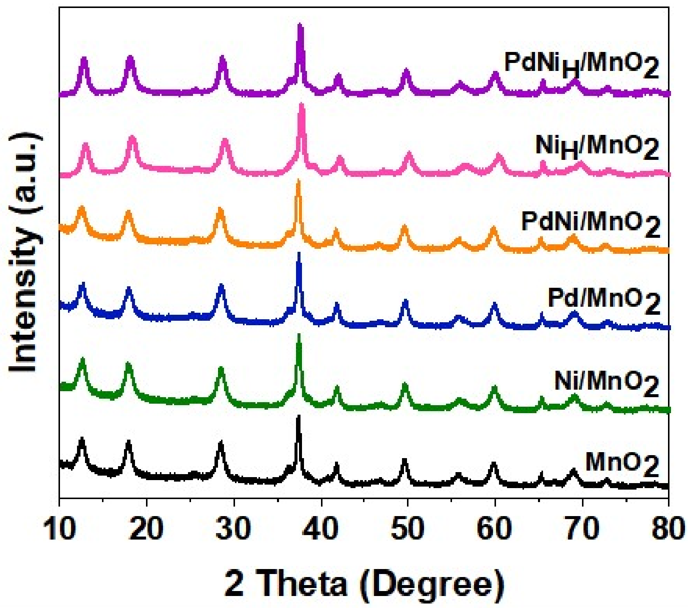

Figure S4. XRD pattern of the prepared catalysts.

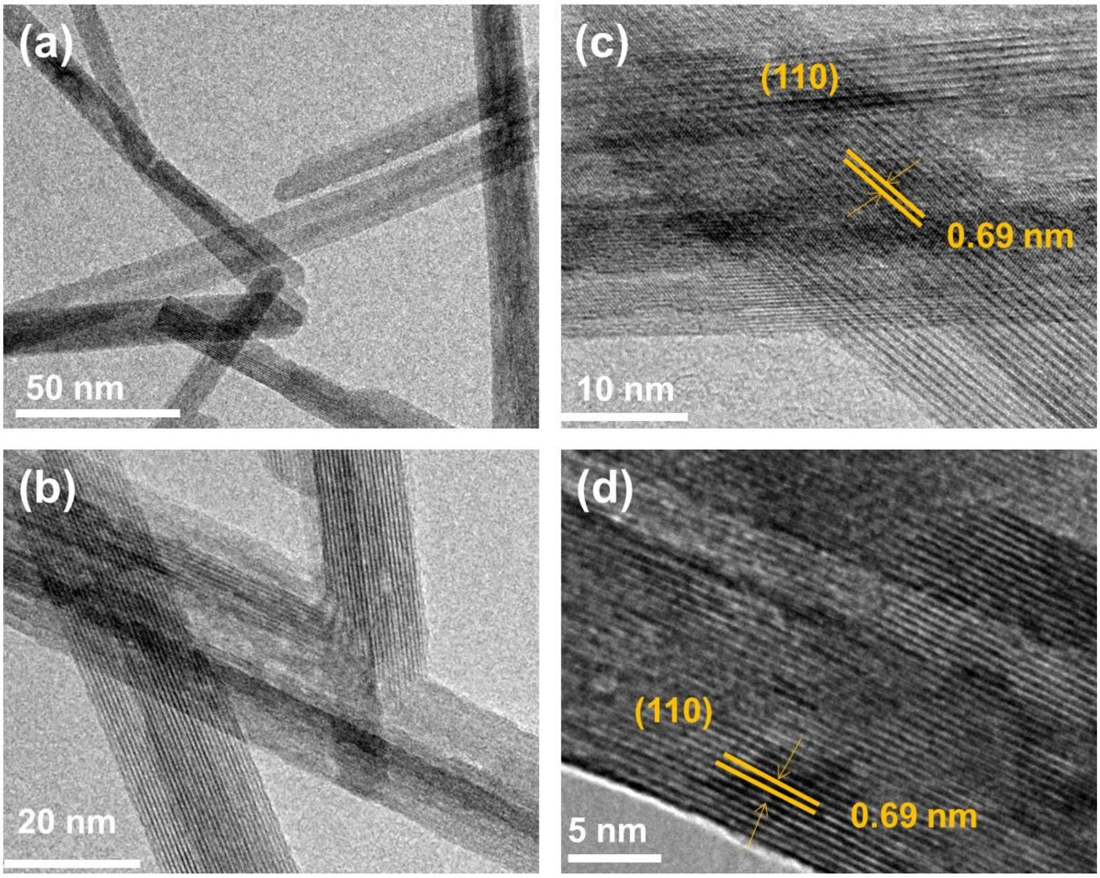

Figure S5. (a-b) TEM and (c-d) HRTEM images of PdNi/MnO_2.

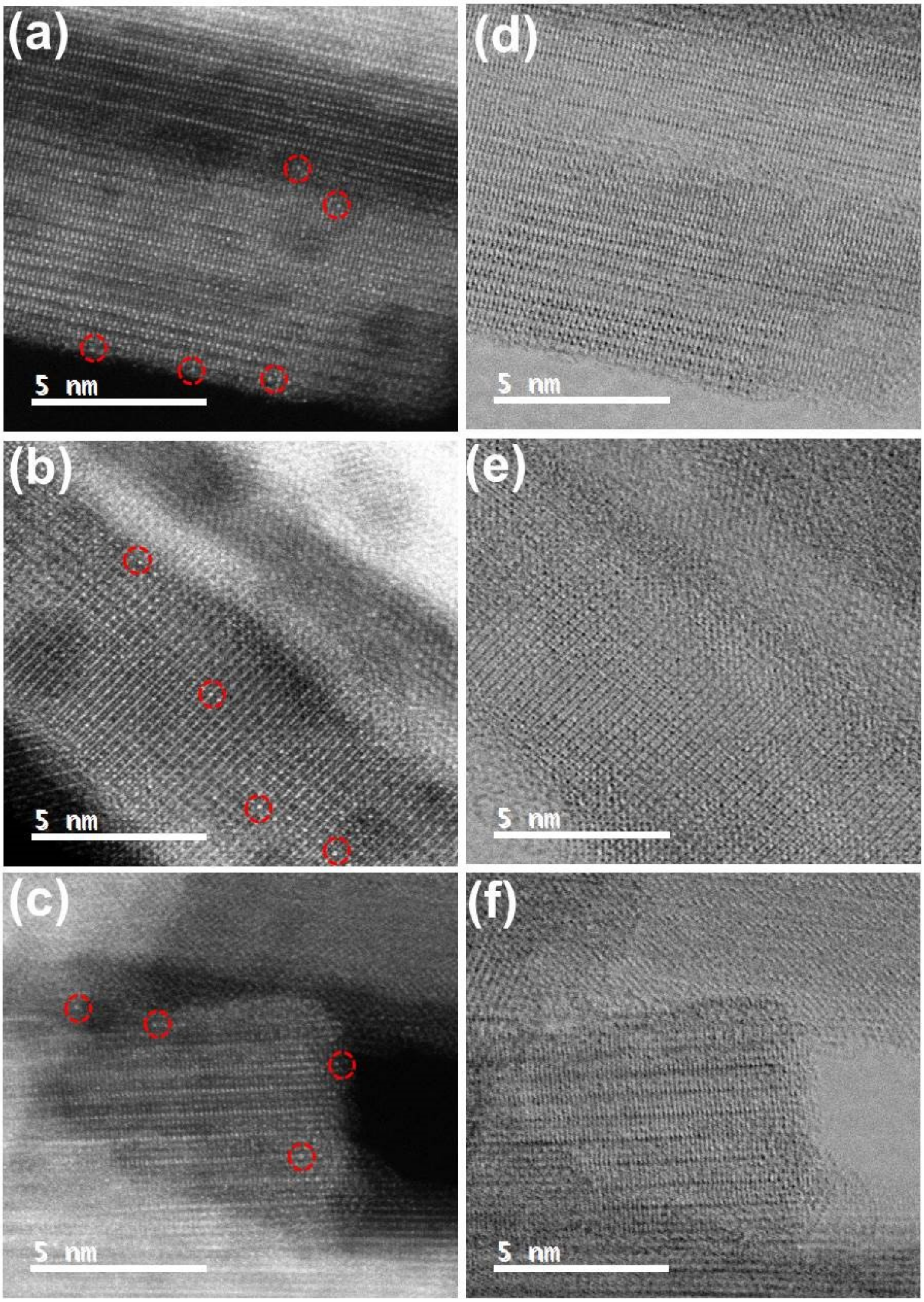

Figure S6. (a-c) HAADF-STEM images and the corresponding ABF-STEM images of PdNi/MnO_2. Red dotted circle highlights the presence of single Pd atom.

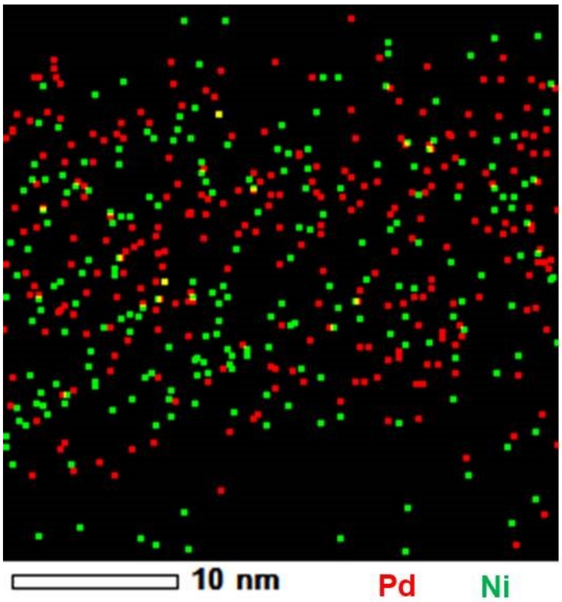

Figure S7. EDS mapping image of integrated Pd and Ni elements

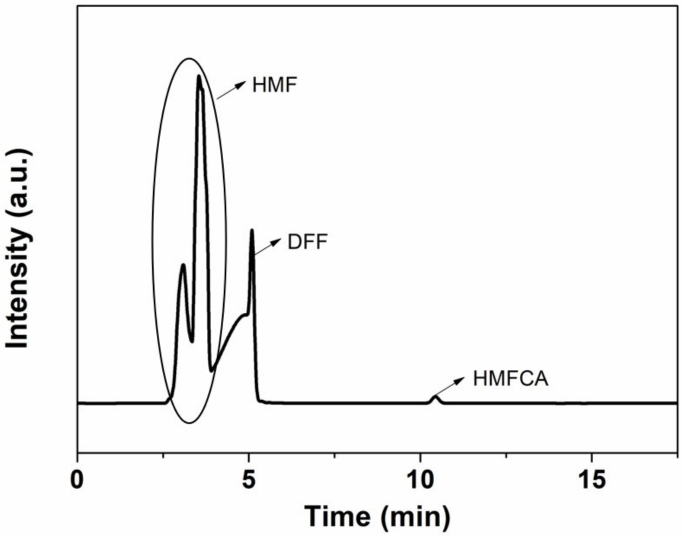

Figure S8. HPLC spectra of the product distribution on MnO_2.

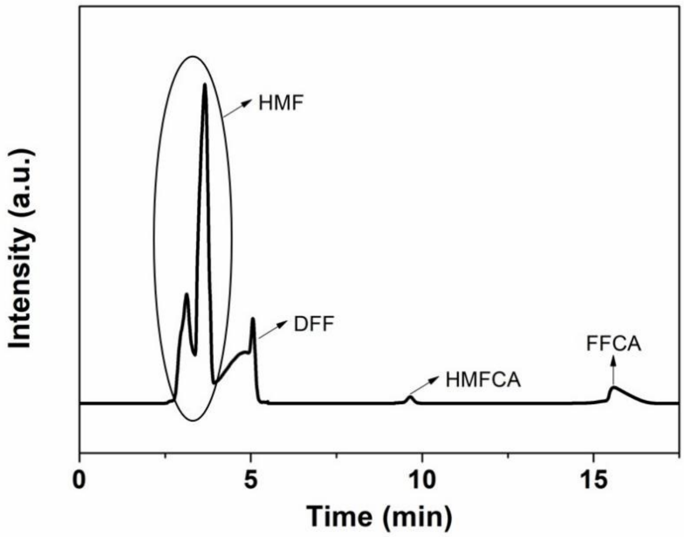

Figure S9. HPLC spectra of the product distribution on Pd/MnO_2.

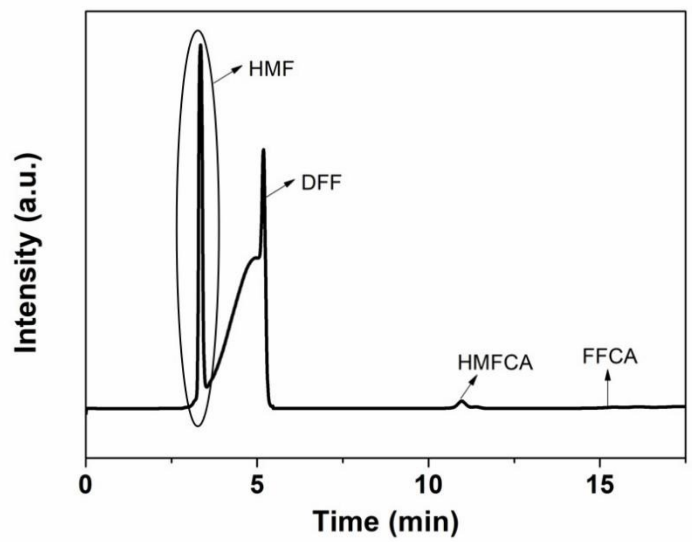

Figure S10. HPLC spectra of the product distribution on Ni/MnO_2.

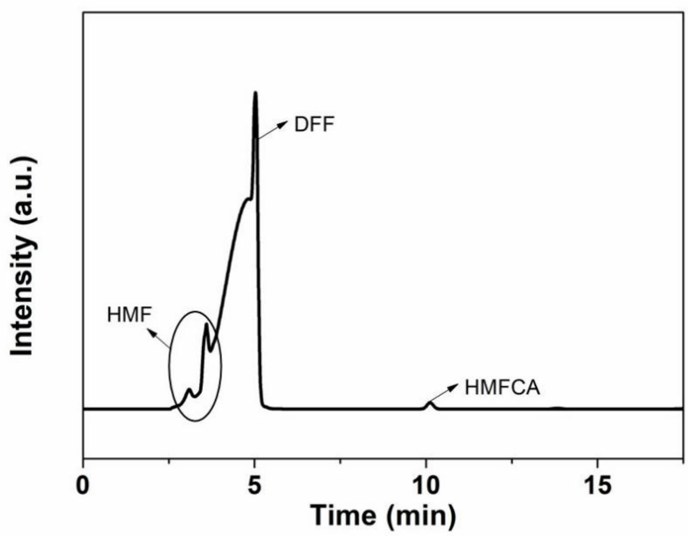

Figure S11. HPLC spectra of the product distribution on PdNi/MnO_2.

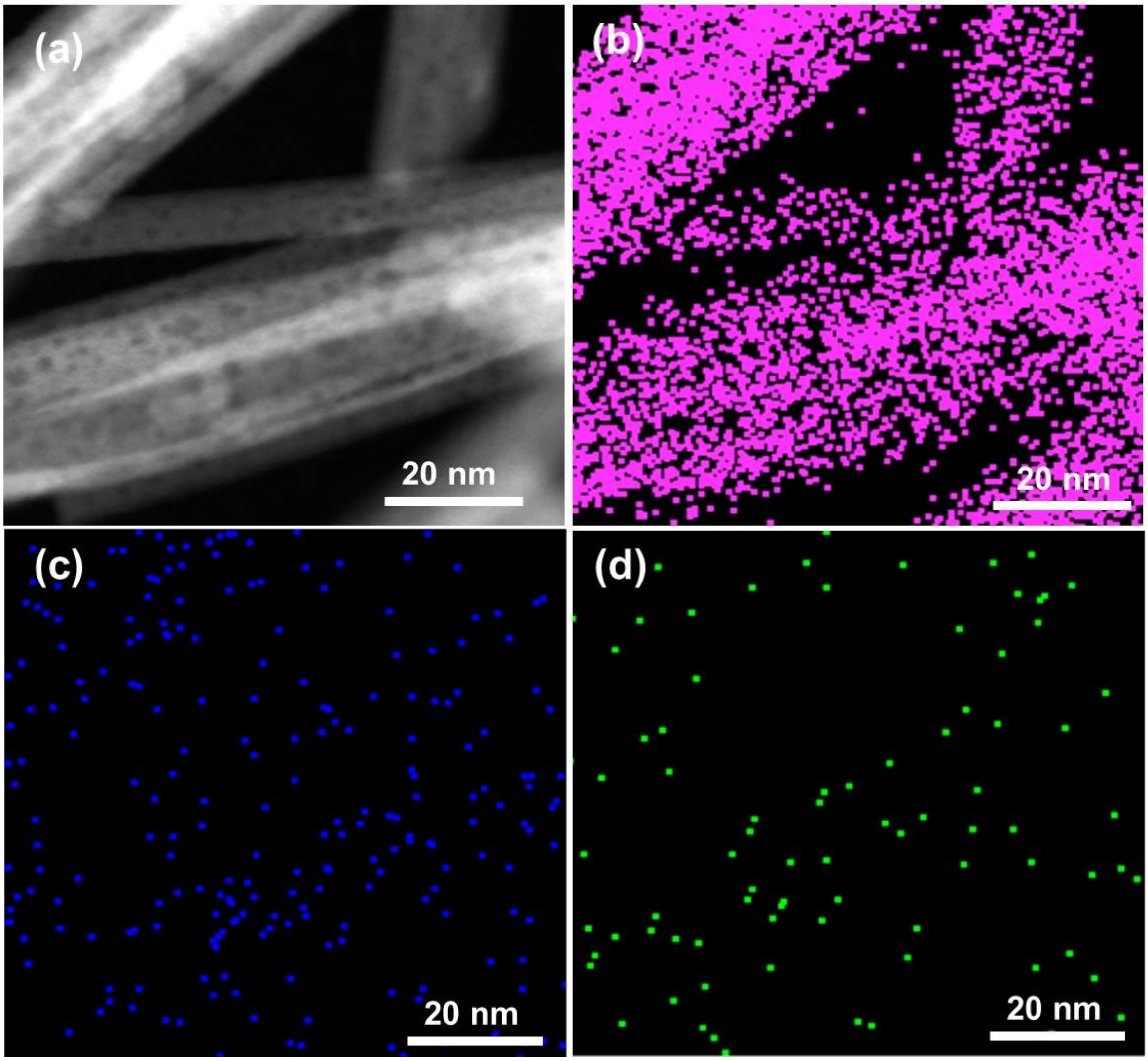

Figure S12. HADDF-STEM images of PdNi/MnO_2 after catalytic recycle measurement. (a) dark field image; (b) Mn signal; (c) Pd signal; (d) Ni signal.

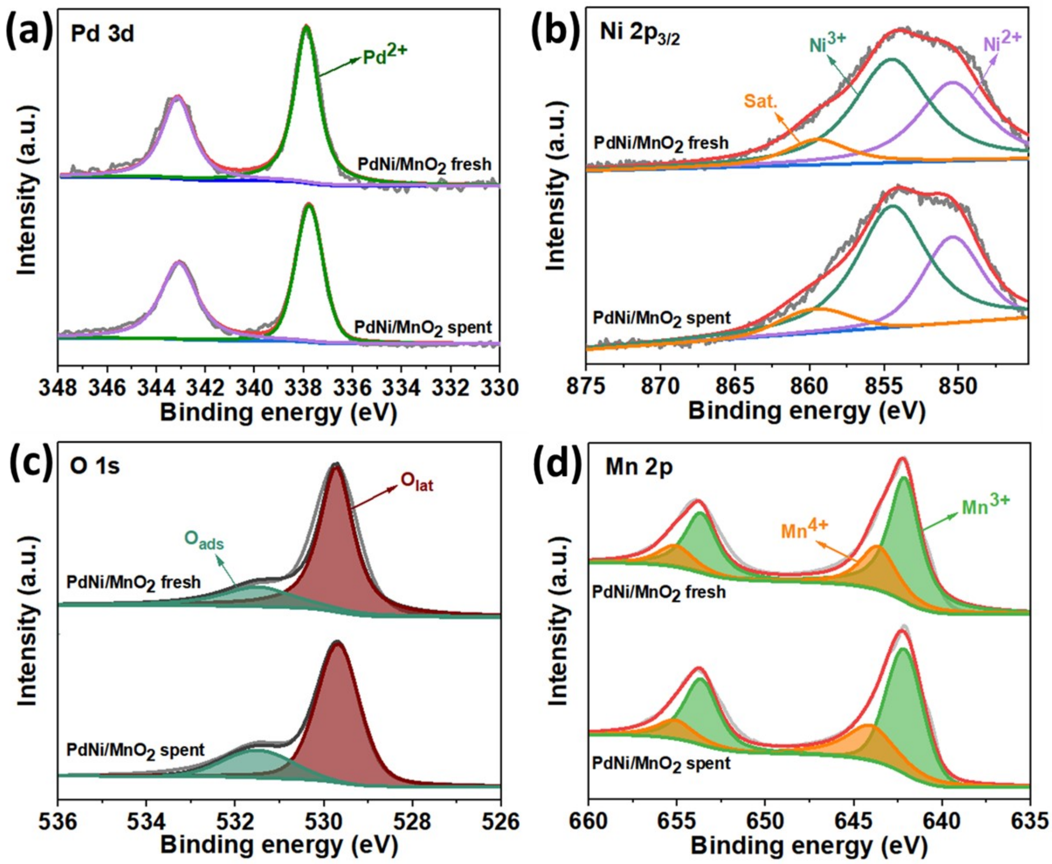

Figure S13. XPS results of the spent and fresh PdNi/MnO_2 catalysts.

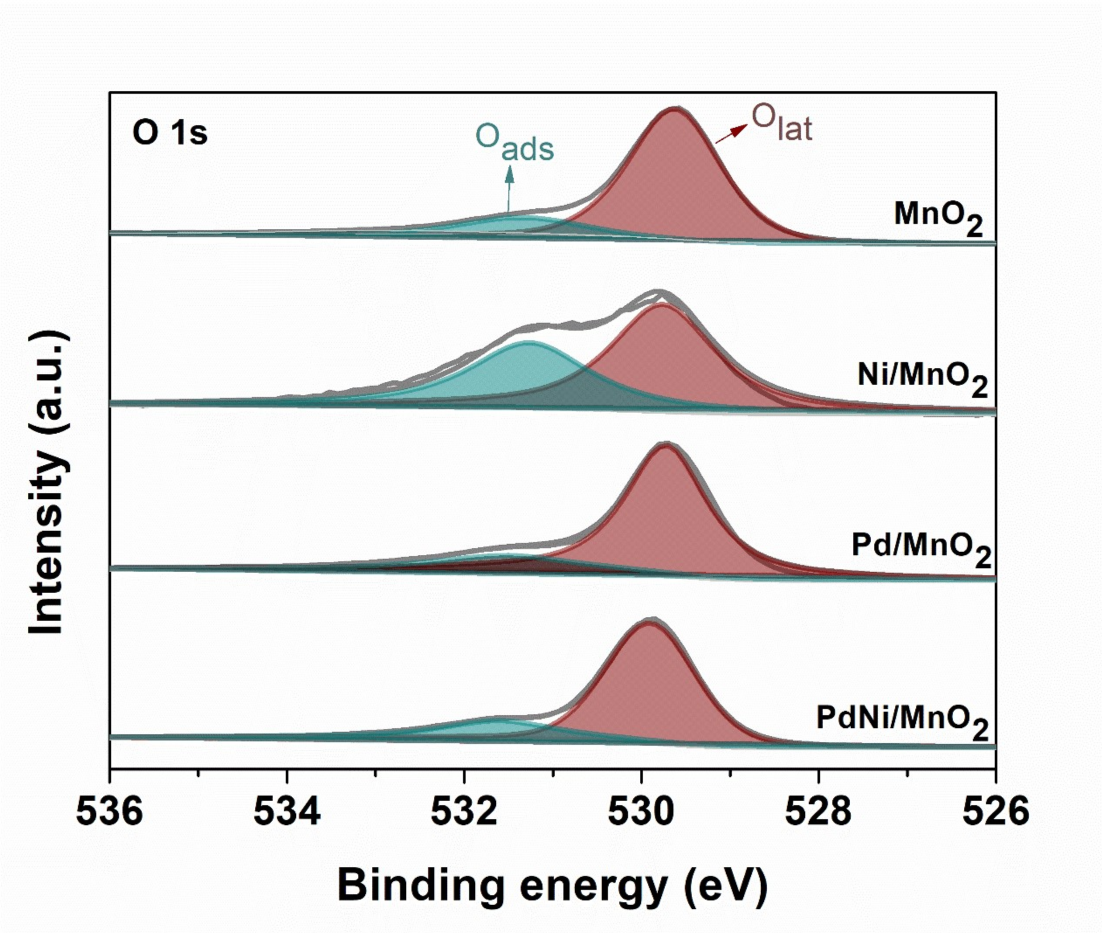

Figure S14. The high-resolution XPS spectrum of O 1s for the prepared catalysts.

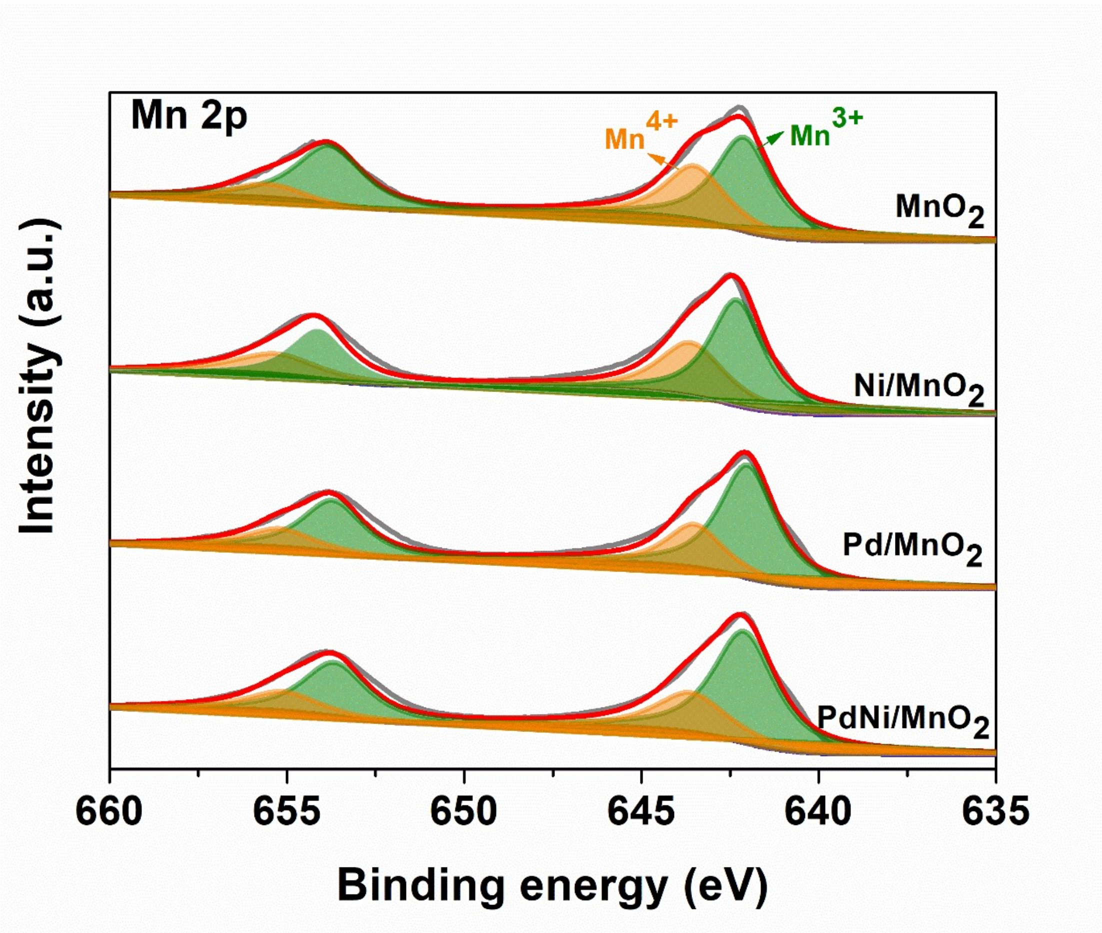

Figure S15. The high-resolution XPS spectrum of Mn 2p for the prepared catalysts.

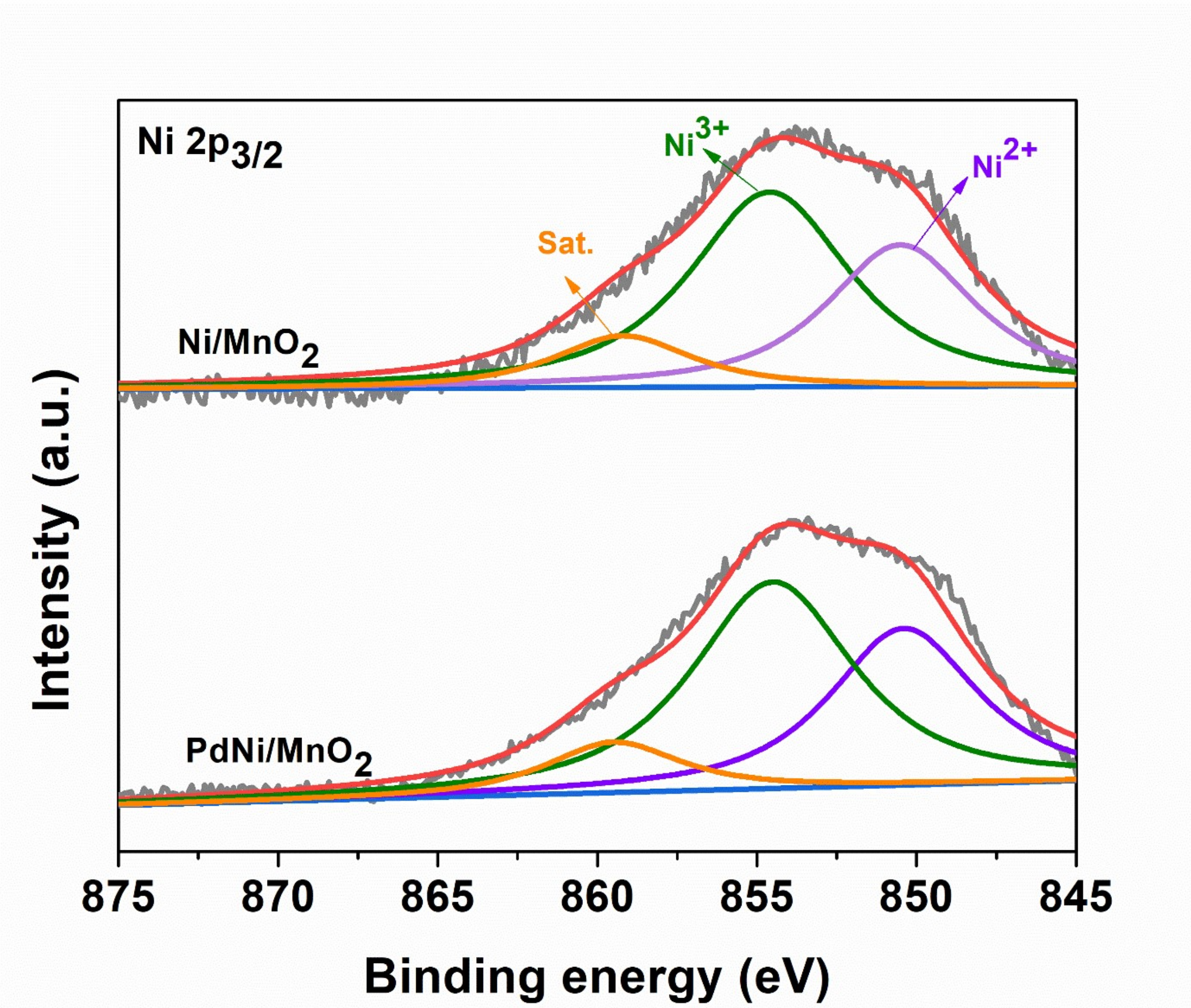

Figure S16. The high-resolution XPS spectrum of Ni $2p_{3/2}$ for the prepared catalysts.

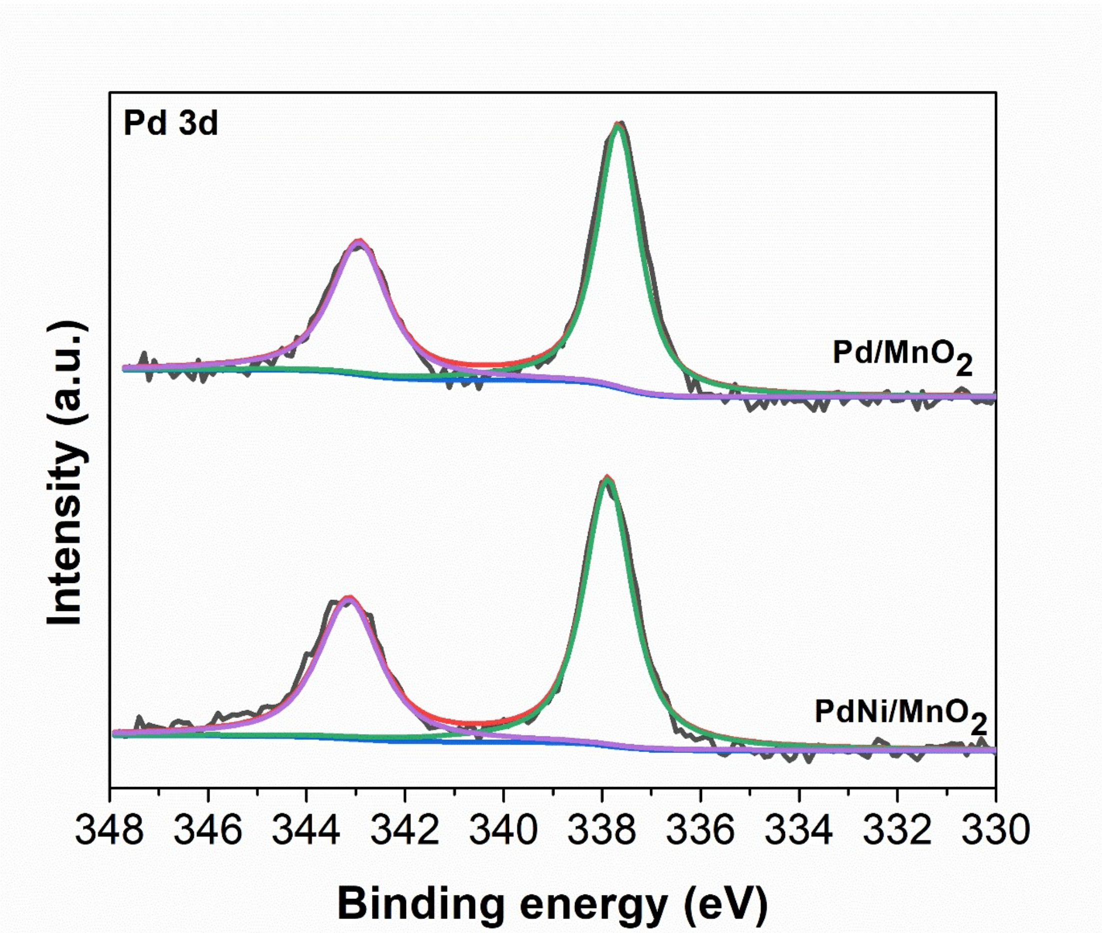

Figure S17. The high-resolution XPS spectra of Pd 3d for the prepared catalysts.

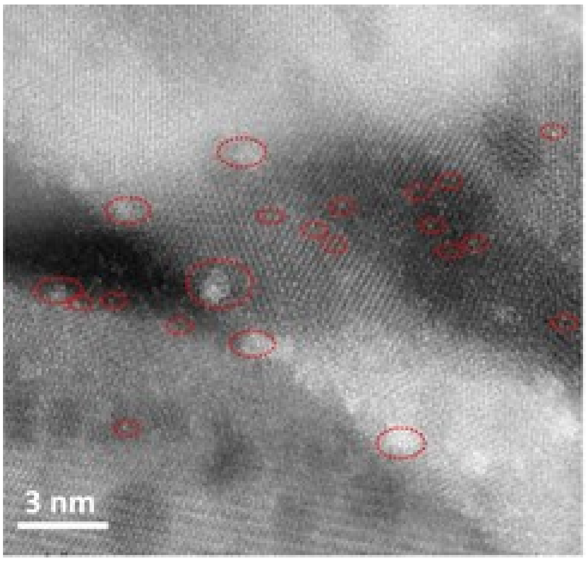

Figure S18. HAADF-STEM images of Pd_H/MnO_2. The white dots highlighted with red circles are Pd sub-nanoclusters. The figures are adopted from our previous publication *J. Energy Chem. 2021, 62, 136-144.*

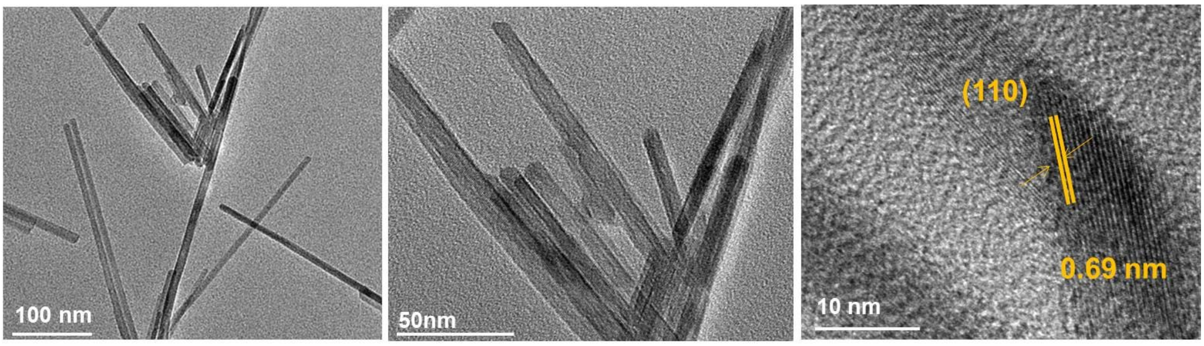

Figure S19. HRTEM images of $NiPd_H/MnO_2$ prepared by hydrothermal method.

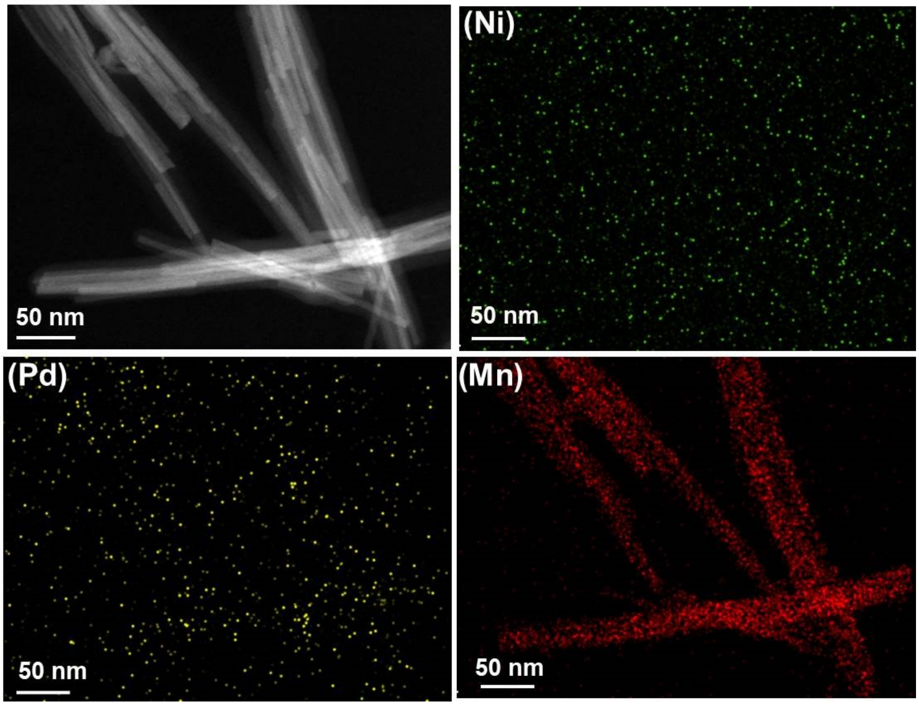

Figure S20. STEM image and corresponding EDS element mapping images of Ni, Pd and Mn elements for $PdNi_H/MnO_2$.

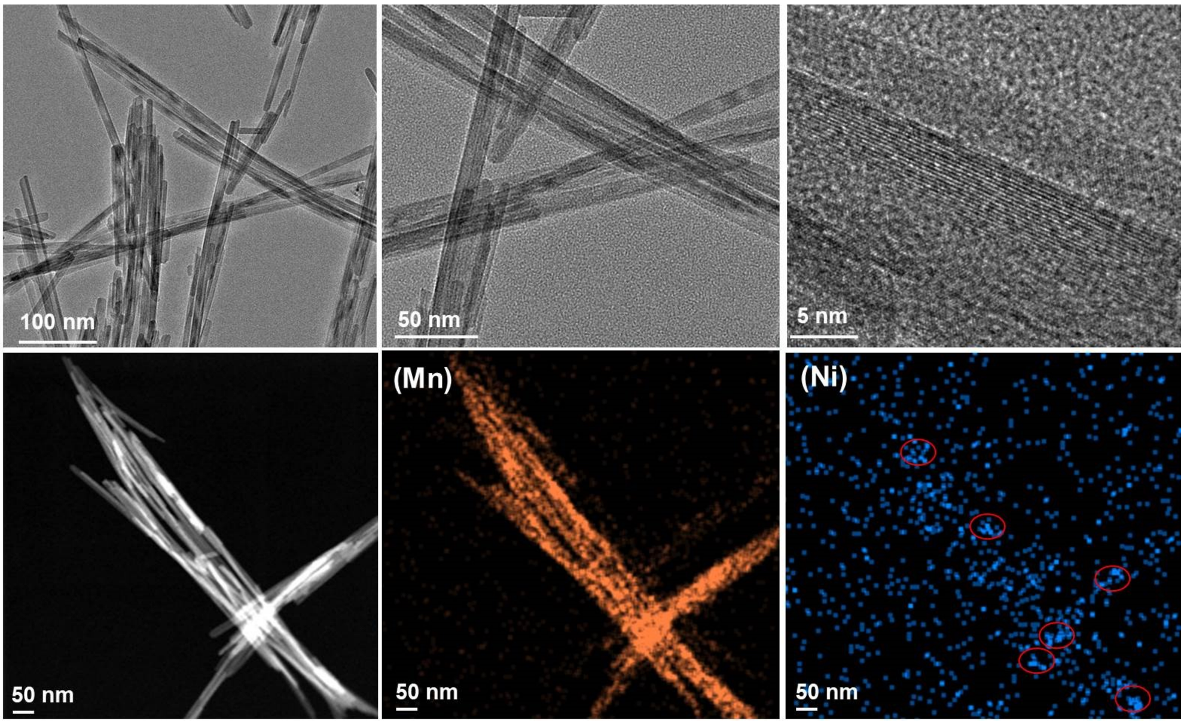

Figure S21. STEM image and corresponding EDS element mapping images of Ni and Mn elements for Ni_H/MnO_2.

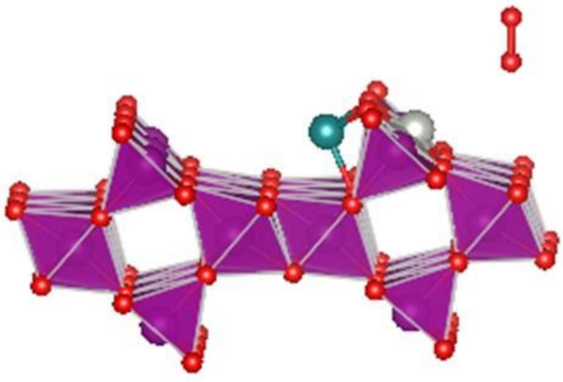

$$\Delta E_{ads}^{O_2}(\mathrm{Pd}) = -0.25\ \mathrm{eV}$$

Figure S22. The stable adsorption models of O_2 molecules on Pd site of $PdNi/MnO_2$-C.

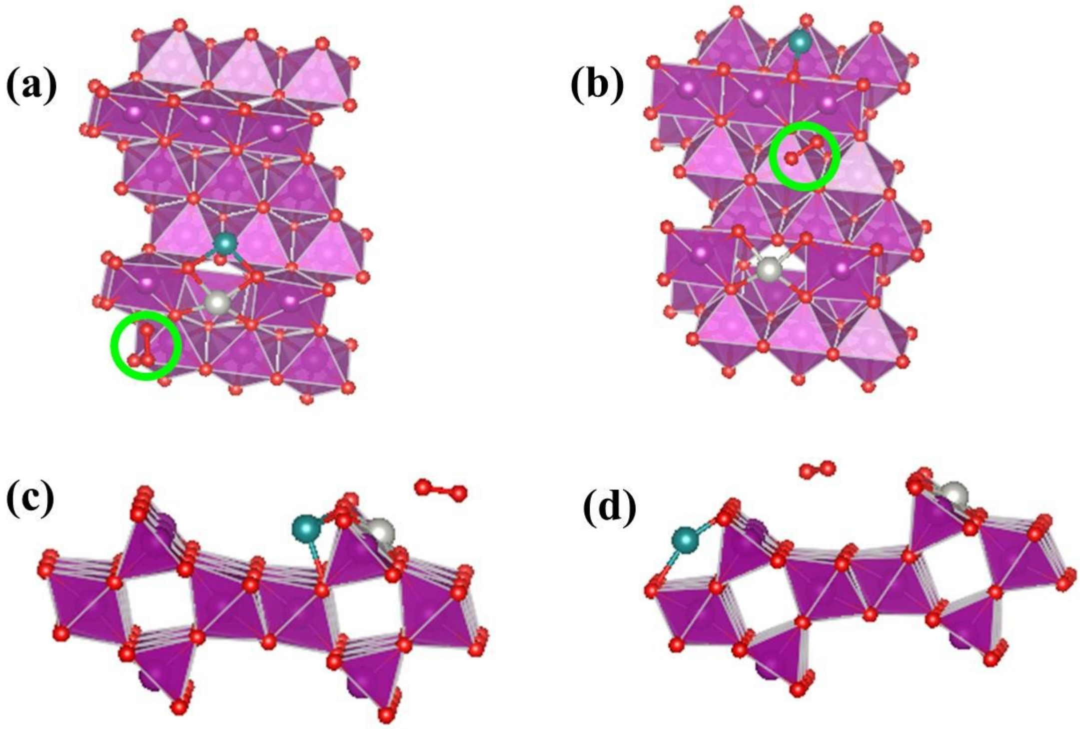

$\Delta E_{ads}^{O_2}$(Mn) = -0.56 eV $\Delta E_{ads}^{O_2}$(Mn) = -0.56eV

Figure S23. The stable adsorption models of O_2 molecules on Mn site of PdNi/MnO_2-C by (a-b) top-view and (c-d) side-view. The green circled is oxygen molecule.

Table S1. Comparison reaction rates on different Mn, Pd, and Ru based catalysts, as well as single atom catalyst for HMF oxidation to DFF.

Entry	Catalyst	Conv. HMF (%)	Yield. DFF (%)	$T_{Reaction}$ (°C)	Time (h)	Oxidant (MPa)	Productvity ($mmol_{DFF}$• g_{cat}^{-1}•h^{-1})	Refs.
1	PdNi-MnO_2	100	>99	120	1	O_2, 1.5	6.34	This work
2	Au-Pd/MnO_2	76.0	74.5	90	6	O_2, 0.1	0.84	[1]
3	1.54%Pd/HCN-900	95.6	94.6	120	6	O_2, 0.1	3.15	[2]
4	MnOx/P25-600-5h	33.2	32.2	140	2	Air, 3.0	1.61	[3]
5	Ru/$MnCo_2O_4$	98.3	98.3	130	3	O_2, 1.0	4.37	[4]
6	α-MnO_2	93.2	78.6	140	4	O_2, 0.5	3.93	[5]
7	Ni_3Mn-LDH	82.3	75.1	100	4	O_2, 0.1	0.94	[6]
8	Ru_1/NiO	91.1	74.1	110	2	O_2, 1.0	0.46	[7]
9	Ru/OMC-P0.56	100	88.0	90	4	O_2, 2.0	5.50	[8]
10	$CoMn_2O_4$-2:3	41.6	41.6	100	2	O_2, 0.8	2.08	[9]
11	g-Fe_2O_3@HAP-Ru	100	89.1	90	4	O_2, 0.1	1.18	[10]
12	Ru/g-Al_2O_3	99.0	96.0	120	4	O_2, 0.28	0.60	[11]
13	Ru/C	100	95.8	110	4	O_2, 2.0	5.99	[12]
14	Ag-OMS-2	99.0	99.0	165	4	Air, 1.5	0.83	[13]
15	Cs/MnOx	98.4	94.7	100	4	O_2, 1.0	5.92	[14]

Table S2. Surface composition of Mn and O species determined from XPS analysis.

Catalyst	Binding energy (eV)			Mn species (%)		O Species (%)	
	Ni $2p_{3/2}$		Pd 3d	Mn 2p		O 1s	
	Ni^{2+}	Ni^{3+}	Pd^{2+}	Mn^{3+}	Mn^{4+}	O_{ads}	O_{lat}
PdNi/MnO_2 fresh	850.4	854.5	337.9	71.0	29.0	22.3	77.7
PdNi/MnO_2 spent	850.4	854.4	337.8	72.3	27.7	21.9	78.1

Table S3. Metal doping contents and catalytic data of Ni_H/MnO_2, Pd_H/MnO_2, and $PdNi_H/MnO_2$。

Catalyst	ICP (Pd%)	ICP (Ni/%)	XPS (Pd/%)	XPS (Ni/%)	Conv. (%)	Yield (%)			Productivity ($mmol_{DFF}.g_{cat}^{-1}.h^{-1}$)
						DFF	HMFCA	Others	
$PdNi_H/MnO_2$	0.45	0.13	-	-	100	71	4	24	4.50
Pd_H/MnO_2	1.70		-	-	51	32	6	13	2.03
Ni_H/MnO_2	-	2.61	-	-	82	23	14	45	1.46

Reaction conditions: $m_{HMF}/m_{catalyst}$ =0.8; 20 ml of 1, 4-dioxane; 1.5 MPa of O_2; T = 120 °C; t= 1h

References

[1] Y.Q. Zhu, M. Lu, *RSC. Adv.*, **2015**, 5, 85579.
[2] Y.Y. Zhu, F.S. Wang, M.Y. Fan, Q. Zhu, Z.P. Dong, *J. Colloid. Interf. Sci*., **2019**, 553, 588.
[3] L.F. Chen, W.Y. Yang, Z.Y. Gui, S. Saravanamurugan, A. Riisager, W.R. Cao, Z.W. Qi, *Catal. Today*, **2019**, 319, 105.
[4] D.K. Mishra, J.K. Cho, Y.J. Kim, *J. Ind. Eng. Chem.*, **2018**, 60, 513-519.
[5] L.H. Yu, H. Chen, Z. Wen, M.M. Jin, Z.W. Ma, X.L. Ma, Y.S. Sang, M.M. Chen, Y.D. Li, *Catal. Today*, **2021**, 367, 9.
[6] W.Y. Zhou, Z.J. Kong, Z. Wu, S. Yang, Y. Wang, Y.P. Liu, *Catal. Commun.*, **2021**, 151.106279.
[7] Y.F. Liu, T. Gan, Q. He, H. Zhang, X.H. He, H.B. Ji, *Ind. Eng. Chem. Res.*, 2020, 59, 4333
[8] M. Hong, S.Y. Wu, J.T. Li, J. Wang, L.F. Wei, K. Li, *Catal. Commun.*, **2020**, 136, 105909.
[9] L. Ding, W.Y. Yang, L.F. Chen, H.Y. Cheng, Z.W. Qi, Catal Today, 347 (2020) 39-47.
[10] Z.H. Zhang, Z.L. Yuan, D.G. Tang, Y.S. Ren, K.L. Lv, B. Liu, *Chemsuschem*, **2014**, 7, 3496.
[11] C.A. Antonyraj, J. Jeong, B. Kim, S. Shin, S. Kim, K.Y. Lee, J.K. Cho, *J. Ind. Eng. Chem*., **2013**, 19 , 1056.
[12] J.F. Nie, J.H. Xie, H.C. Liu, *J. Catal*., **2013**, 301, 83.
[13] G.D. Yadav, R.V. Sharma, *Appl. Catal. B-Environ*, **2014**, 147, 293.
[14] Z.L. Yuan, B. Liu, P. Zhou, Z.H. Zhang, Q. Chi, *Catal. Sci. Technol*., **2018**, 8, 4430.